ORGANIC CHEMISTRY

FRONTIERS

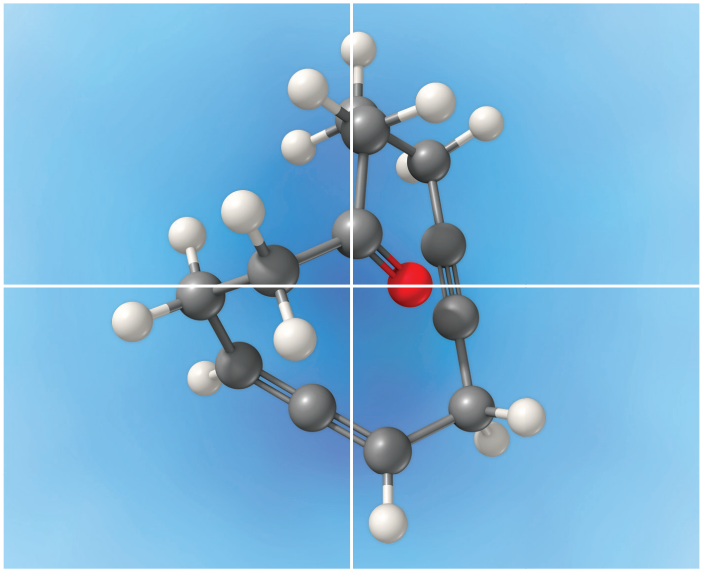

Accepted Manuscript

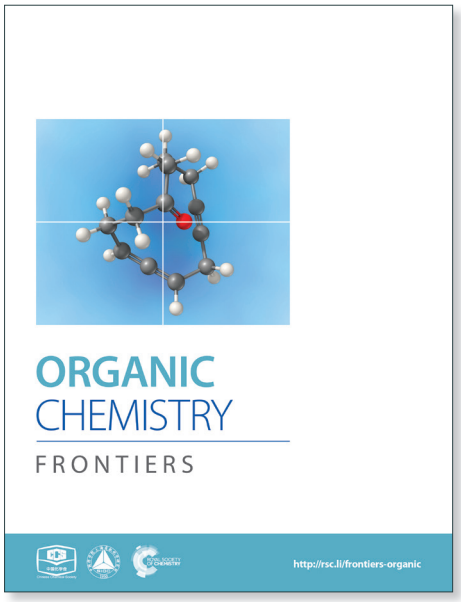

This is an *Accepted Manuscript*, which has been through the Royal Society of Chemistry peer review process and has been accepted for publication.

Accepted Manuscripts are published online shortly after acceptance, before technical editing, formatting and proof reading. Using this free service, authors can make their results available to the community, in citable form, before we publish the edited article. We will replace this *Accepted Manuscript* with the edited and formatted *Advance Article* as soon as it is available.

You can find more information about *Accepted Manuscripts* in the **Information for Authors**.

Please note that technical editing may introduce minor changes to the text and/or graphics, which may alter content. The journal's standard **Terms & Conditions** and the **Ethical guidelines** still apply. In no event shall the Royal Society of Chemistry be held responsible for any errors or omissions in this *Accepted Manuscript* or any consequences arising from the use of any information it contains.

Cite this: DOI: 10.1039/c0xx00000x

www.rsc.org/xxxxxx

ARTICLE TYPE

Density Functional Study on the Mechanism of Direct *N*-Acylation Reaction of Lactams with Aldehydes Catalyzed by Shvo's Catalyst

Qian Liu,[a] Xi Lu,[*b,c] Xiaomin Sun[d] and Xian Zhao[*a]

Received (in XXX, XXX) Xth XXXXXXXXX 20XX, Accepted Xth XXXXXXXXX 20XX
DOI: 10.1039/b000000x

Abstract: Density functional theory (DFT) was used to explore the mechanism of the direct *N*-acylation of lactam with aldehyde under the catalysis of Shvo's catalyst. A most kinetically and thermodynamically feasible mechanism was proposed in this study. The lactam-lactim tautomerism was firstly achieved by means of a concertedly intermolecular hydrogen exchange between two molecules of 2-pyrrolidinone, **1**. Then, the formed lactim **2** and aldehydes reacted to obtain a hemiaminal **3** via a nucleophilic reaction and a hydrogen transfer. Finally, the product **5** was generated using a dehydrogenation of the hemiaminal **3** catalyzed under ruthenium complex **4**. The total Gibbs energy barrier is 23.9 kcal/mol in the catalytic cycle of *N*-acylation, and the generation of the hemiaminal **3** is the rate-determining step.

Introduction

Due to significantly biological activity,[1] *N*-acylated lactams, oxazolidinones and imidazolidinones are widely applied in natural products and medication.[2-6] Thus, an effective and economic method is urgent and essential to the synthesis of these amides compounds. As previous reports, a classical method of *N*-acylation reaction is employing acyl chlorides or anhydrides with the aid of alkyl lithium reagents.[7] Some facile approaches were subsequently further developed such as the *N*-acylated oxazolidinones using acid fluorides and mild bases like iPr$_2$NEt and NEt$_3$ (Scheme 1),[8] and the copper-catalyzed C-H activation of aldehydes with amides in the presence of *N*-bromosuccinimide (NBS) (Scheme 2).[9]

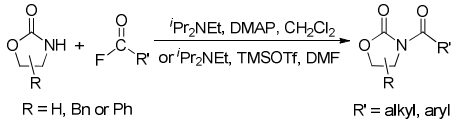

Scheme 1. The *N*-acylation reaction of oxazolidinone using acid fluorides.

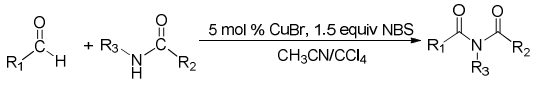

Scheme 2. Directly copper-catalyzed amidation of aldehydes in the presence of NBS.

Although these improved methods make the synthetic process more facile and convenient, the rigorous reaction conditions are difficult to be achieved and the stoichiometric reagents are also expensive for the bulk producing. By comparisons, the reported transition-metal-catalyzed oxidative amidation of aldehydes with amines has a desired atom economical transformation,[10-16] due to a much higher catalytic dehydrogenated efficiency. Recently, Zhang and Hong demonstrated a direct method on *N*-acylations of lactams, oxazolidinones, and imidazolidinones with aldehydes catalyzed by Shvo's catalyst without any stoichiometric reagent (Scheme 3),[17,18,19] which also showed a great functional tolerance for substrates. This enhancement is more "green" for environment and more atom-economical for synthesis cost. More recently, Lei *et al.* also successfully developed an iron catalyzed coupling reaction between aldehydes and amides, which possibly involves a radical process (Scheme 4).[20]

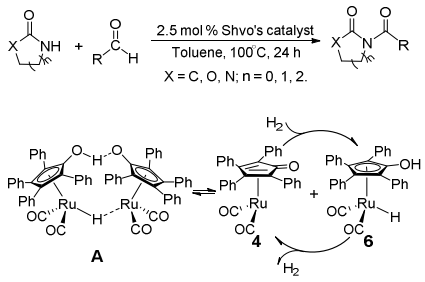

Scheme 3. Direct *N*-acylations of lactams, oxazolidinones, and imidazolidinones with aldehydes are achieved under the catalysis of Shvo's catalyst **A**.

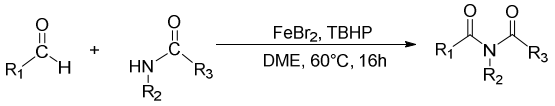

Scheme 4. An oxidative C–H/N–H coupling of aldehydes with simple amides catalyzed by an iron catalyst.

However, to further develop a wider application of *N*-acylation reaction and the appreciable range of substrates, only depending on experiment is very difficult and expensive considering the synthesis time of substrates and catalysts. Here a deep and detailed study of the mechanism and the elementary steps involved with the direct *N*-acylation of lactams, oxazolidinones, and imidazolidinones with aldehydes is offered as a prerequisite for the further improvement. Density functional theory (DFT) was used to perform a detailed theoretical study for the mechanism of Zhang and Hong's method. The calculated results were then analyzed to clarify relationships between structures and reactivities in order to supply more reliable and available information to experiment.

Computational details

To obtain a more reasonable computational result, the substrates of 2-pyrrolidinone and benzaldehyde derive from Zhang and Hong's experiments.[17] The original structure of Shvo's catalyst **A** is also used here without any simplification.[18] All optimizations were performed at the density functional theory (DFT) level by means of the M06-2X functional. Zhao and Truhlar reported that the M06-2X method can get a high accuracy for the calculation of the thermochemistry and kinetics of transition metals and main-group elements.[21,22] Besides, the effective core potential LANL2DZ[23] along with its associated basis set was employed for ruthenium and the main group elements (C, O, H, and Si) were calculated using the 6-31G* basis set. All calculations were performed without any geometrical constraints. Frequency calculations were done for all stationary points under the same computational level in order to identify the minima (zero imaginary frequency) and transition states (TS, only one imaginary frequency) and to provide Gibbs energies at 298.15 K and 1 atm. Intrinsic reaction coordinate (IRC)[24] analysis was carried out to confirm that all stationary states were smoothly connected to each other. Solvent effects (in toluene) were included using the SMD model[25,26] with the same method by performing single-point calculations via the optimized-geometries in gas phase at the higher level of basis set, where the def2-TZVP basis set was employed for Ru and the 6-31++G** basis set was used for main group elements.[27,28] A correction term of 1.8943 kcal/mol must be added to the *G*(sol) calculations to convert the gas-phase standard Gibbs energies at a standard state of 1 atm to the appropriate standard state for a solution of 1 mol/L.[29,30] Solvation Gibbs energies Δ*G*(sol) were used to explore the reaction mechanism in order to consider both entropic and solvent effects. Calculations for all geometries were carried out using the Gaussian 09 software package.[31]

Results and Discussion

The acylation mechanism via unimolecular lactam. According to Zhang and Hong's proposal,[17] *N*-acylation of lactams was possibly achieved via a unimolecular nucleophilic attacking mechanism (Scheme 5). In this route, the 2-pyrrolidinone **1** firstly transforms to the lactim **2** via an intramolecular lactam-lactim tautomerism. Then a nucleophilic attack of lactim **2** to the carbonyl group of aldehyde generates a hemiaminal intermediate **3**, which can be further dehydrogenated with the help of ruthenium complex **4**. Finally, the acylation product **5** and another ruthenium species **6** are produced by *β*-hydride elimination and proton transfer.

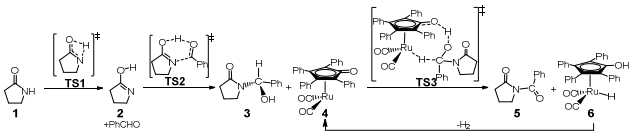

Scheme 5. The unimolecular nucleophilic acylation mechanism.

Figure 1 shows that the substrate **1** transfers to the lactim **2** via the transition state **TS1** with a very high Gibbs energy barrier of 50.5 kcal/mol. In this intramolecular lactam-lactim tautomerism, the bond angle of OCN is firstly reduced to 110º in the transition state **TS1** from 126º in the substrate **1** in order to hydrogen atom transfer to carbonyl oxygen from nitrogen. Moreover, the H-N bond length was enlarged to 1.325 Å, whereas the H-O distance was shortened to 1.360 Å. Here the four-member ring of OHNC was shaped like a diamond, by which an exceedingly high ring strain force was correspondingly induced in geometry of **TS1**. Thus the Gibbs energy barrier of the first step was significantly enhanced. Although the geometry of **2** did not cause an intramolecular geometric stain, its thermodynamic stability was still reduced due to the activated *N*-atom.

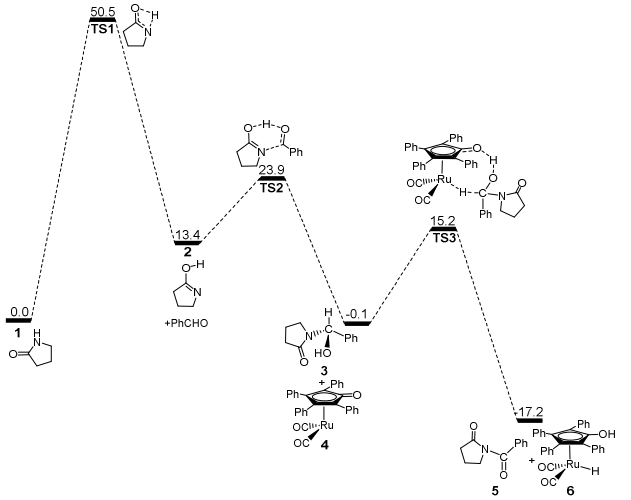

Figure 1. Gibbs energy Δ*G*(sol) profiles (kcal/mol) for the acylation mechanism via unimolecular lactam. Relative to Gibbs energies of **1**, PhCHO and **4**.

In the next step the lactim **2** reacted with the carbonyl carbon of benzaldehyde, where the corresponding transition state **TS2** had a Gibbs energy barrier of 10.5 kcal/mol. From the structure of **TS2**,

the N-C bond length of 1.896 Å indicates that the *N*-atom is attacking the carbonyl carbon atom. Besides, two H-O bond lengths of 1.036 and 1.508 Å correspond to hydroxyl hydrogen concertedly transferring to the oxygen of PhCHO. After this process, a hemiaminal intermediate **3** was then formed and its geometry resembled a tetrahedron (Figure 2). Here, the **1** + PhCHO → **3** reaction was exergonic by 0.1 kcal/mol, which indicated this hemiaminal **3** owning a better thermodynamic stability compared with the reactants of **1** and PhCHO. This is also in agreement with the experimental results.[17]

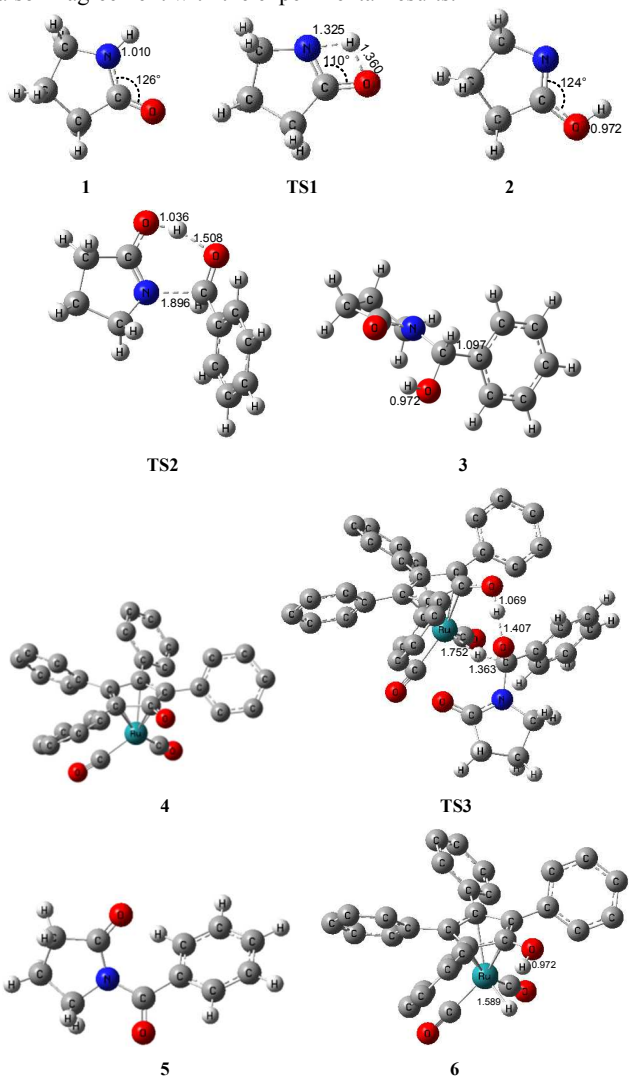

Figure 2. Optimized structures for the acylation via unimolecular lactam. Distances in Å. Hydrogen atoms of Cp group of Shvo's catalyst omitted for clarity.

Due to the presence of Shvo's catalyst, an oxidized ruthenium complex **4** can be generated following the dissociation of the diruthenium-bridging hydride.[32-37] Thus the hemiaminal **3** can be further hydrogenated under the catalysis of ruthenium complex **4**. According to numerous of experimental and theoretical studies,[38-42] the concerted hydrogen transfer mechanism was demonstrated to be a most thermodynamically and kinetically reasonable pathway. From the transition state **TS3**, two bond distances of O···H−O (1.069 Å) and Ru···H−C (1.752 Å) indicate that two hydrogen atoms of CH−OH of **3** are concertedly transferring to the oxygen atom of CpO substituent and the ruthenium center of **4** by means of the format of proton and hydride ion, respectively. The Gibbs energy barrier $\Delta G^{\neq}$(sol) was 15.3 kcal/mol for the **3** + **4** → **5** + **6** reaction, which was exergonic by 17.1 kcal/mol.

For this mechanism, the other processes are kinetically and thermodynamically facile reaction except the first step. However, the initial intramolecular lactam-lactim tautomerism causes a large Gibbs energy barrier of 50.5 kcal/mol, due to the very large structural strain force. This barrier cannot be kinetically overcome under the experimental conditions, because it is generally required to heat up to a very high temperature which far exceeds the boiling point of toluene.

Ruthenium-mediated acylation mechanism. As above mentioned, a ruthenium complex **4** can exist in the reaction system after the dissociation of Shvo's catalyst. Due to having an unoccupied d-orbital, the Ru-complex **4** is also a very good electron acceptor. As a donor, the substrate **1** possibly forms another ruthenium complex **7** by providing the carbonyl oxygen atom to the vacant site of ruthenium of **4**. Scheme 6 shows that this complexing reaction is exergonic by 10.1 kcal/mol, although there is an entropic penalty. In Ru-complex **7** (see Figure 3), there is also a hydrogen bonding interaction between oxygen of Cp-ring group and H-N of 2-pyrrolidinone besides a coordination bond, due to the distance of O···HN being 1.878 Å. Both facts are favorable to increase the thermodynamic stability of Ru-complex **7**. This means that the substrate **1** is possibly captured by Ru-complex **4** due to a higher thermodynamic stability of Ru-complex **7**.

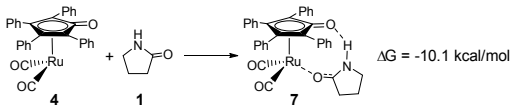

Scheme 6. The complexing reaction between Ru-complex **4** and substrate **1**.

Next, the intramolecular lactam-lactim tautomerism occurs with the aid of ruthenium coordination using the transition state **TS4**. From the geometries of **TS4**, there is also a four-ring straining impact as **TS1**. In addition, the protophilia of oxygen of substrate **1** is also reduced due to coordination to ruthenium compared with **TS1**. So the Gibbs energy barrier is increased to a higher value of 55.5 kcal/mol (see Figure 4). Compared with the structure of **7**, the bond length of O−Ru is nearly increased by 0.1 Å, which indicates the O−Ru coordination bond being impaired. This causes the intermediate **7** becoming more thermodynamically unstable, which the process of **7** → **8** is correspondingly endergonic by 21.2 kcal/mol.

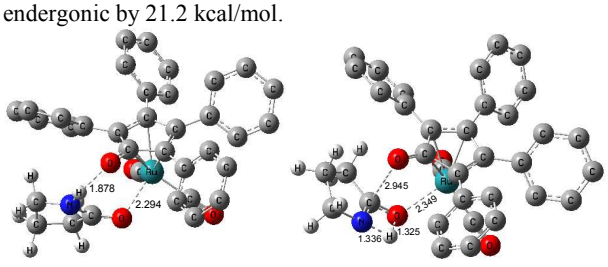

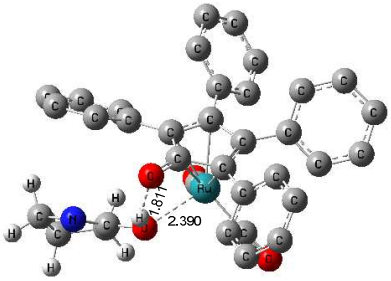

8

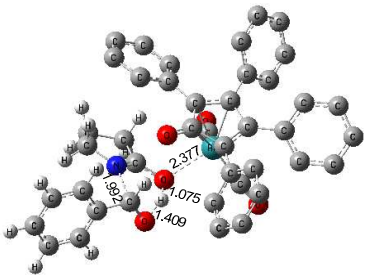

TS5

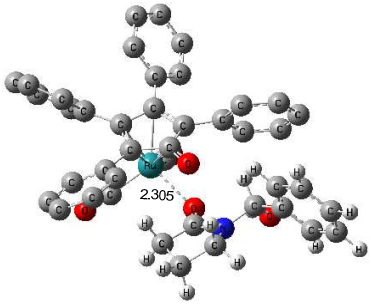

9

Figure 3. Optimized structures for ruthenium-mediated acylation mechanism. Distances in Å. Hydrogen atoms of Cp group of Shvo's catalyst omitted for clarity.

The further nucleophilic attacking and hydrogen transfer between **8** and PhCHO can produce the hemiaminal-ruthenium complex **9** via transition state **TS5** with a Gibbs energy barrier of 14.4 kcal/mol, which is higher than 10.5 kcal/mol of **2** → **TS2**. It is because the coordinated ruthenium complex induces a steric hinderance when PhCHO closes to substrate. This fact eventually gives rise to the thermodynamic stability reducing of hemiaminal-ruthenium complex **9**, of which the Δ*G*(sol) is increased to 5.2 kcal/mol compared with the reactants of **1** and PhCHO.

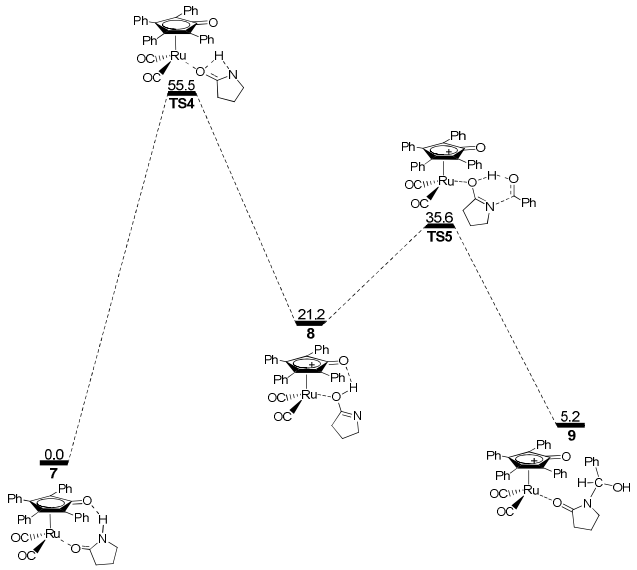

Figure 4. Gibbs energy Δ*G*(sol) profiles (kcal/mol) for ruthenium-mediated acylation mechanism. Relative to Gibbs energies of **7** and PhCHO.

By far, the participation of ruthenium complex does not display an expected action in acylation of lactam with aldehyde. In contract, the total Gibbs energy barrier of this route and Δ*G*(sol) of product **9** are increased to 55.5 kcal/mol and 5.2 kcal/mol, respectively, which indicates this mechanism being kinetically and thermodynamically unfeasible. From this mechanism, it can be found that the substrate **1** can coordinate to Ru-complex **4** and form a ruthenium complex **7** prior to the lactam-lactim tautomerism when Shvo's catalyst is added to the reaction system. However, the generation of Ru-complex **7** is unfavorable to the further catalytic dehydrogenation reaction.

Bimolecular lactams participated acylation mechanism. To avoid the geometric straining, there is actually another potential means that the lactam-lactim tautomerism is achieved via an intermolecular hydrogen exchange between two substrates **1**. As shown in Figure 5, two molecules of lactam **1** exchange two hydrogen atoms each other via the transition state **TS6** having a six-membered ring, which only corresponds to a Gibbs energy barrier of 10.5 kcal/mol. Figure 6 shows that the geometry of **1** is retained to a large extent in the transition state **TS6**. So this indicates that the intermolecular hydrogen exchange can effectively eliminate the straining impact.

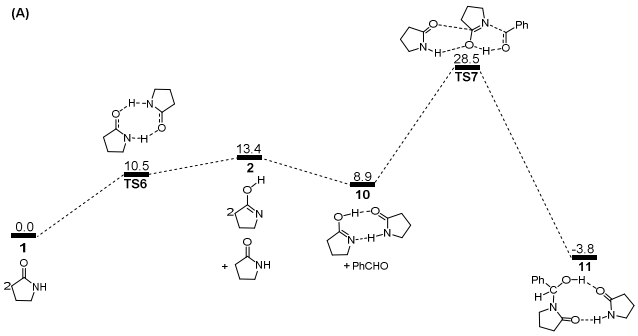

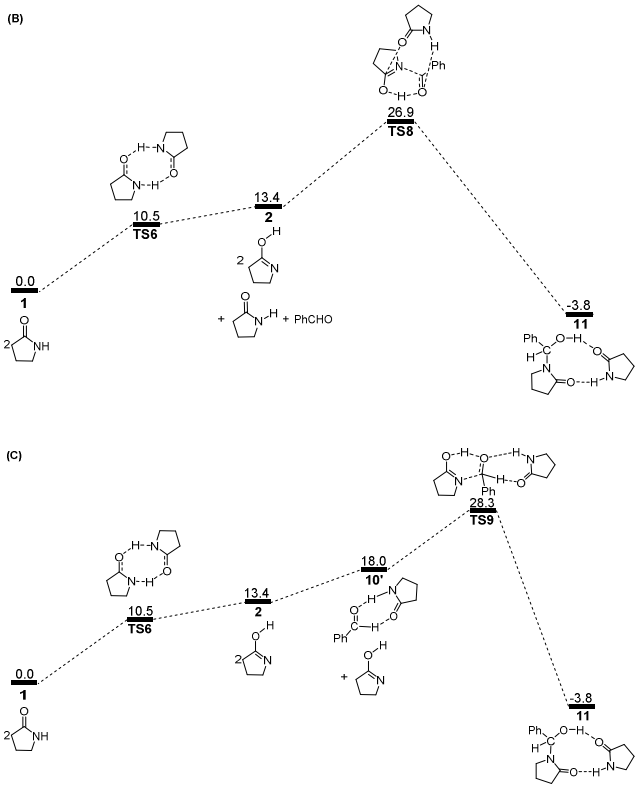

Figure 5. Gibbs energy ΔG(sol) profiles (kcal/mol) for bimolecular lactams participated acylation mechanisms: (a) formed a bimolecular intermediate via **1** and **2** before **TS7**; (b) has a bimolecular structure in **TS8**; (c) formed a bimolecular intermediate between **1** and **PhCHO** before **TS9**. Relative to Gibbs energies of **1** and PhCHO.

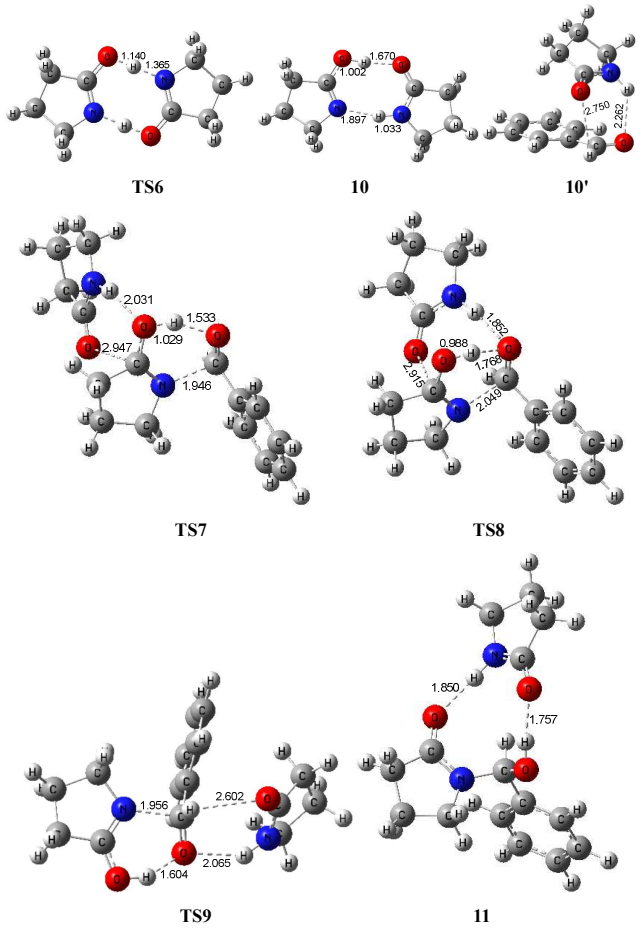

Figure 6. Optimized structures for bimolecular lactams participated acylation mechanism. Distances in Å.

Correspondingly, two lactims **2** are also generated through the transition state **TS6**, which was endergonic by 13.4 kcal/mol from **1** to **10**. In particular, Gibbs energy of the produced lactim **2** is 2.9 kcal/mol higher than that of **TS6**. As Shaik's theory,[43] the reaction of **1** → **TS6** → **2** is a continued endothermic process, where the real Gibbs energy should be 13.4 kcal/mol instead of 10.5 kcal/mol. In this case, a more stable intermediate **10** is then generated with a exergonic 4.5 kcal/mol from **2** to **10**. The intermediate **10** is actually a bimolecular complex involved with the lactim **2** and lactam **1**. Figure 6 shows that the OH···O and N···HN distances are 1.670 and 1.897 Å, respectively. This indicates two strong hydrogen bonding interaction formed in **10**, which is favorable to improve the thermodynamic stability.

However, there are three possible pathways (a), (b) and (c) in the next step, which corresponds to three different transition states **TS7**, **TS8** and **TS9,** respectively. In these transition states, the function of substrate **1** is mainly used to increase both the electropositivity of carbon and the electronegativity of oxygen that participate in the nucleophilic reaction. By comparisons, the transition state **TS8** in the (b) route corresponds to a lowest Gibbs energy barrier of 26.9 kcal/mol, where the oxygen of PhCHO is more favorable to accept the proton from the OH of **10**. Then an intermediate **11** was produced, which is a molecular pair of the hemiaminal **3** and substrate **1** connected by hydrogen bonds.

The total Gibbs energy barrier is 26.9 kcal/mol from **1** to **11** in this mechanism, which is exergonic by 3.8 kcal/mol. Compared with **1** → **TS1** → **2** of the first route, a bimolecular hydrogen exchange via **TS6** is much more kinetically feasible to achieve the lactam-lactim tautomerism. This calculated conclusion is also in agreement with the previous theoretical and experimental results[44]. Although the finally produced molecular pair **11** also has a higher thermodynamic stability compared with a single hemiaminal **3**, the Gibbs energy barrier of **TS8** is 3.0 kcal/mol higher than that of **TS2**. Thus, the unimolecular **2** is more kinetically favorable to make a nucleophilic attacking to PhCHO. This means that the dimer **10** is again dissociated to the monomer **2**, and then lactim **2** further produces the hemiaminal **3** via **TS2**.

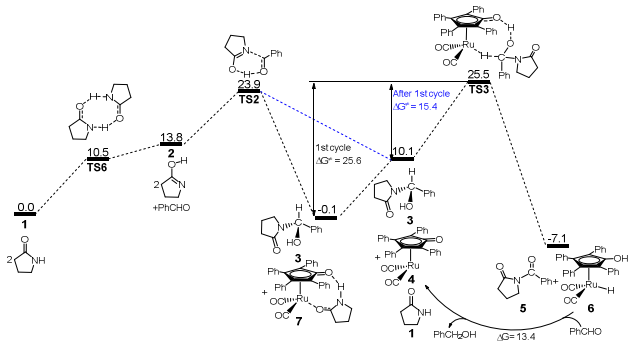

Figure 7. Gibbs energy Δ*G*(sol) profiles (kcal/mol) for the most reasonable acylation mechanism. Relative to Gibbs energies of **1**, PhCHO, and **7**.

According to above analyses, the most reasonable mechanism is shown in Figure 7. Here the Gibbs energy shows an increasing tendency for **1** → **TS1** → **2** + PhCHO → **TS2**, which is a continuously endergonic process.[43] So the actual Gibbs energy barrier is 23.9 kcal/mol for the generation of hemiaminal **3**. Adding Shvo's catalyst with substrates into the reaction system can cause an higher Gibbs energy barrier of 25.6 kcal/mol for the first catalytic cycle, due to forming a more thermodynamically stable Ru-complex **7**. After the first cycle, the Ru-complex **6** is initially regenerated to the active catalyst **4**,[28] and then the following dehydrogenation of hemiaminal can be directly catalyzed by the Ru-catalyst **4**. It is because a lower Gibbs energy barrier of 15.4 kcal/mol has a preponderant kinetic favorableness compared with Ru-complex **7**. Here Gibbs energy barrier of hemiaminal formation is 23.9 kcal/mol which is higher than 15.3 kcal/mol of dehydrogenation of **3**. This means that the rate-determining step is **2** + PhCHO → **TS2** → **3** in the real catalytic cycle, which is also in agreement with experimental results. The total Gibbs energy barrier becomes 23.9 kcal/mol for the *N*-acylation of lactam with aldehyde. Furthermore, the crucial factor on further developing this method is improving the nucleophilicity of lactams or the electrophilic ability of aldehydes according to this mechanism.

Conclusions

The mechanism of the direct *N*-acylation of lactam with aldehyde under Shvo's catalyst was studied using DFT method in detail. Solvation effects in toluene were also considered and were included in calculated Gibbs energy profiles. In the acylation process, the substrate **1** can isomerize to the lactim 2 by means of an intermolecular lactam-lactim tautomerism. The formed monomer **2**, which can generate to a hemiaminal **3** with aldehydes via a nucleophilic reaction and a hydrogen transfer. Finally, this hemiaminal **3** is dehydrogenated to obtain the product **5** under the catalysis of ruthenium complex **4**. The highest Gibbs energy barrier is 23.9 kcal/mol for the catalytic cycle, where the generation of the hemiaminal **3** is the rate-determining step. In paricular, adding Shvo's catalyst into substrates can increase the Gibbs energy barrier for the first cycle of *N*-acylation. Besides, increasing the nucleophilicity of lactams or the electrophilic ability of aldehydes is favorable to further develop this synthesis method.

Acknowledgement

This work is supported by National Natural Science Foundation of China (No. 21277082 and 21337001), Marie Curie International Research Staff Exchange Scheme Fellowship within the 7th European Community Framework Programme (No. 295132) and Program for New Century Excellent Talents in University (NCET-13-0349).

Notes and references

[a] *State Key Laboratory of Crystal Materials, Shandong University, Jinan 250100, China; E-mail: zhaoxian@sdu.edu.cn.*
[b] *Department of Chemical and Materials Engineering, University of Alberta, Edmonton, AB, T6G 2V4, Canada; E-mail: xlu2@ualberta.ca.*
[c] *Research Institute of Petroleum Exploration and Development, Sinopec, Beijing, 100083, People's Republic of China.*
[d] *Environment Research Institute, Shandong University, Jinan, 250100, People's Republic of China.*

† Electronic Supplementary Information (ESI) available: [Total electronic energies, thermal corrections to Gibbs energies and Cartesian coordinates, and so on]. See DOI:

Keywords: *N*-acylation; lactam; ruthenium complex; hemiaminal; mechanism.

1 (a) T. Cupido, J. Tulla-Puche, J. Spengler, F. Albericio, *Curr. Opin. Drug Discovery Dev.* 2007, **10**, 768–783. (b) J. W. Bode, *Curr. Opin. Drug Discovery Dev.* 2006, **9**, 765–775.
2 J. M. Humphrey, A. R. Chamberlin, *Chem. Rev.* 1997, **97**, 2243–2266.
3 (a) K. Hayashi, K. Nunami, J. Kato, N. Yoneda, M. Kubo, T. Ochiai, R. Ishida, *J. Med. Chem.* 1989, **32**, 289–297. (b) D. M. Robinson, M. P. Curran, K. A. Lyseng-Williamson, *Drugs* 2007, **67**, 1359–1378.
4 (a) M. Sakakiba, M. Matsui, *Agric. Biol. Chem.* 1973, **37**, 911–914. (b) A. Ishida, T. Mukaiyama, *Bull. Chem. Soc. Jpn.* 1978, **51**, 2077–2081.
5 (a) G. Bandoli, M. Nicolini, H. Lumbroso, A. Grassi, G. C. Pappalardo, *J. Mol. Struct.* 1987, **160**, 297–309. (b) C. M. Tang, Q. Y. Shi, A. Katchman, G. Lynch, *Science* 1991, **254**, 288–290.
6 C. Y. Li, W. Tsai, A. G. Damu, E. J. Lee, T. S. Wu, N. X. Dung, T. D. Thang, L. Thanh, *J. Agric. Food Chem.* 2007, **55**, 9436–9442.
7 (a) A. Giovannini, D. Savoia, A. Umani-Ronchi, *J. Org. Chem.* 1989, **54**, 228–234. (b) D. Savoia, V. Concialini, S. Roffia, L. Tarsi, *J. Org. Chem.* 1991, **56**, 1822–1827.
8 C. S. Schindler, P. M. Forster, E. M. Carreira, *Org. Lett.* 2010, **12**, 4102–4105.
9 L. Wang, H. Fu, Y. Y. Jiang, Y. F. Zhao, *Chem.-Eur. J.* 2008, **14**, 10722–10726.
10 W.-J. Yoo, C.-J. Li, *J. Am. Chem. Soc.* 2006, **128**, 13064–13065.
11 (a) Y. Suto, N. Yamagiwa, Y. Torisawa, *Tetrahedron Lett.* 2008, **49**, 5732–5735. (b) Y. Tamaru, Y. Yamada, Z. Yoshida, *Synthesis* 1983, 474–476.
12 (a) A. Tillack, I. Rudloff, M. Beller, *Eur. J. Org. Chem.* 2001, **2001**, 523–528. (b) W.-K. Chan, C.-M. Ho, M.-K. Wong, C.-M. Che, *J. Am. Chem. Soc.* 2006, **128**, 14796–14797.
13 T. Naota, S.-I. Murahashi, *Synlett* 1991, **1991**, 693–694.
14 (a) S. Seo, T. J. Marks, *Org. Lett.* 2008, *10*, 317–319. (b) C. Qian, X. Zhang, J. Li, F. Xu, Y. Zhang, Q. Shen, *Organometallics* 2009, **28**, 3856–3862.
15 J. M. Li, F. Xu, Y. Zhang, Q. Shen, *J. Org. Chem.* 2009, **74**, 2575–2577.
16 S. Muthaiah, S. C. Ghosh, J. E. Jee, C. Chen, J. Zhang, S. H. Hong, *J. Org. Chem.* 2010, **75**, 3002–3006.
17 J. Zhang, S. H. Hong, *Org. Lett.* 2012, **14**, 4646–4649.
18 Y. Shvo, D. Czarkie, Y. Rahamim, D. F. Chodosh, *J. Am. Chem. Soc.* 1986, **108**, 7400–7402.
19 (a) R. Karvemu, R. Prabhakaran, K. Natarajan, *Coord. Chem. Rev.* 2005, **249**, 911−918. (b) S. Gladiali, E. Alberico, *Chem. Soc. Rev.* 2006, **35**, 226–236.
20 J. Wang, C. Liu, J. Yuan, A. Lei, *Chem. Comm.* 2014, **50**, 4736–4739.

21 Y. Zhao, D. G. Truhlar, *Acc. Chem. Res.* 2008, **41**, 157–167.
22 Y. Zhao, D. G. Truhlar, *Theor. Chem. Acc.* 2008, **120**, 215–241.
23 (a) P. J. Hay, W. R. Wadt, *J. Chem. Phys.* 1985, **82**, 270–283; (b) P. J. Hay, W. R. Wadt, *J. Chem. Phys.* 1985, **82**, 299–310.
24 (a) K. Fukui, *J. Phys. Chem.* 1970, **74**, 4161–4163; (b) K. Fukui, *Acc. Chem. Res.* 1981, **14**, 363–368.
25 A. V. Marenich, C. J. Cramer, D. G. Truhlar, *J. Phys. Chem. B* 2009, **113**, 4538–4543.
26 A. V. Marenich, C. J. Cramer, D. G. Truhlar, *J. Phys. Chem. B* 2009, **113**, 6378–6396.
27 X. Xu, D. G. Truhlar, *J. Chem. Theory Comput.* 2012, **8**, 80–90.
28 X. Lu, Q. Liu, X. Wang, R. Cheng, M. Zhang, X. Sun, *RSC Adv.* 2015, **5**, 2827–2836.
29 L. M. Pratt, S. Merry, S. C. Nguyen, P. Quan, B. T. Thanh, *Tetrahedron* 2006, **62**, 10821–10828.
30 L. M. Pratt, D. G. Truhlar, C. J. Cramer, S. R. Kass, J. D. Thompson, J. D. Xidos, *J. Org. Chem.* 2007, **72**, 2962–2966.
31 Gaussian 09 (Revision B.01), M. J. Frisch, G. W. Trucks, H. B. Schlegel, G. E. Scuseria, M. A. Robb, J. R. Cheeseman, G. Scalmani, V. Barone, B. Mennucci, G. A. Petersson, H. Nakatsuji, M. Caricato, X. Li, H. P. Hratchian, A. F. Izmaylov, J. Bloino, G. Zheng, J. L. Sonnenberg, M. Hada, M. Ehara, K. Toyota, R. Fukuda, J. Hasegawa, M. Ishida, T. Nakajima, Y. Honda, O. Kitao, H. Nakai, T. Vreven, J. A. Montgomery, Jr. J. E. Peralta, F. Ogliaro, M. Bearpark, J. J. Heyd, E. Brothers, K. N. Kudin, V. N. Staroverov, R. Kobayashi, J. Normand, K. Raghavachari, A. Rendell, J. C. Burant, S. S. Iyengar, J. Tomasi, M. Cossi, N. Rega, J. M. Millam, M. Klene, J. E. Knox, J. B. Cross, V. Bakken, C. Adamo, J. Jaramillo, R. Gomperts, R. E. Stratmann, O. Yazyev, A. J. Austin, R. Cammi, C. Pomelli, J. W. Ochterski, R. L. Martin, K. Morokuma, V. G. Zakrzewski, G. A. Voth, P. Salvador, J. J. Dannenberg, S. Dapprich, A. D. Daniels, O. Farkas, J. B. Foresman, J. V. Ortiz, J. Cioslowski,, D. J. Fox, Gaussian, Inc., Wallingford CT, 2009.
32 C. P. Casey, S. W. Singer, D. R. Powell, R. K. Hayashi, M. Kavana, *J. Am. Chem. Soc.* 2001, **123**, 1090–1100.
33 L. S. M. Samec, J.-E. Bäckvall, P. G. Andersson, P. Brant, *Chem. Soc. Rev.* 2006, **35**, 237–248.
34 Clapham, S. E.; Hadzovic, A.; Morris, R. H. *Coord. Chem. Rev.* 2004, **248**, 2201–2237.
35 G. Csjernyk, A. H. Éll, L. Fadini, B. Pugin, J.-E. Bäckvall, *J. Org. Chem.* 2002, **67**, 1657–1662.
36 C. P. Casey, G. A. Bikzhanova, Q. Cui, I. A. Guzei, *J. Am. Chem. Soc.* 2005, **127**, 14062–14071.
37 J. B. Johnson, J.-E. Bäckvall, *J. Org. Chem.* 2003, **68**, 7681–7684.
38 C. P. Casey, H. Guan, *J. Am. Chem. Soc.* 2007, **129**, 5816–5817.
39 C. P. Casey, H. Guan, *Organometallics* 2012, **31**, 2631–2638.
40 A. Comas-Vives, G. Ujaque, A. Lledós, *Organometallics* 2007, **26**, 4135–4144.
41 H. Zhang, D. Chen, Y. Zhang, G. Zhang, J. Liu, *Dalton Trans.* 2010, **39**, 1972–1978.
42 (a) X. Lu, Y. Zhang, P. Yun, M. Zhang, T. Li, *Org. Biomol. Chem.* 2013, **11**, 5264–5277. (b) X. Lu, R. Cheng, N. Turner, Q. Liu, M. Zhang, X. Sun, *J. Org. Chem.* 2014, **79**, 9355−9364.
43 S. Kozuch, S. Shaik, *Acc. Chem. Res.* 2011, **44**, 101–110.
44 (a) S. Tolosa, N. Mora-Diez, A. Hidalgoa, J. A. Sansóna, *RSC Adv.* 2014, **4**, 44757–44768. (b) C. S. Peng, C. R. Baiz, A. Tokmakoff, *Proc. Nat. Acad. Sci.* 2013, **23**, 9243−9248. (c) D. Ray, A. Pramanik, N. Guchhait, *J. Photochem. Photobiol. A Chem.* 2014, **274**, 33–42. (d) H. I. Abdulla, M. F. El-Bermani, *Spectrochimica Acta A* 2001, **57**, 2659–2671.